IR multiphoton photochemistry of CF3Cl

Alexander B. Horwitz, Jack M. Preses, Ralph E. Weston Jr., and George W. Flynn

Citation: The Journal of Chemical Physics **74**, 5008 (1981); doi: 10.1063/1.441753
View online: http://dx.doi.org/10.1063/1.441753
View Table of Contents: http://scitation.aip.org/content/aip/journal/jcp/74/9?ver=pdfcov
Published by the AIP Publishing

IR multiphoton photochemistry of CF_3Cl [a)]

Alexander B. Horwitz, Jack M. Preses, and Ralph E. Weston, Jr.

Department of Chemistry, Brookhaven National Laboratory, Upton, New York 11973

George W. Flynn[b)]

Department of Chemistry, Columbia University, New York, New York 10027
(Received 11 November 1980; accepted 19 January 1981)

CF_3Cl has been dissociated using the focused output of a CO_2 TEA laser operating on the $R(40)$ line of the 9.6 μm band. IR fluorescence has been observed for $HF^\dagger$ and $HCl^\dagger$ after irradiating mixtures of CF_3Cl, HBr, and Ar, indicating the production of F as well as Cl. In addition, the laser-induced fluorescence spectrum of CF_2 has been observed using a KrF laser (249 nm) to excite the $CF_2\ \tilde{A}^1B_1 \leftarrow \tilde{X}^1A_1$ transition. A two-step dissociation mechanism in which CF_3 and Cl are the primary products followed by the subsequent multiphoton absorption and dissociation of CF_3 to produce CF_2 and F is proposed. Evidence for secondary dissociation of CF_3 has been demonstrated by observing CF_2 in the infrared multiphoton dissociation of C_2F_6, which is known to produce CF_3 at low fluence. Further evidence in support of a two-step dissociation mechanism is given by analysis of stable products, fluence studies, and RRKM calculations.

I. INTRODUCTION

Infrared multiphoton dissociation (IRMPD) of halogenated methanes has been studied extensively in recent years.[1-3] These molecules exhibit strong absorption bands in the 9–11 μm region, making them ideal subjects for multiphoton dissociation by the absorption of CO_2 laser radiation. In a number of cases,[4-6] the IRMPD process has been shown to be isotopically specific. However, the relationship between the dissociation mechanism and mode selectivity is still the subject of controversy.[7-9] For example, static-cell experiments on the IRMPD of CF_2Cl_2 and CF_2Br_2 suggest the three-center elimination of Cl_2 and Br_2, respectively, as the primary dissociative step,[10,11] while molecular beam studies indicate that atom elimination primarily occurs.[12]

Elucidation of the mechanism in IRMPD processes is directly dependent upon correct identification of dissociation products. This can often be difficult, especially for large molecules. For low pressure crossed-beam experiments,[1,12] an on-line mass spectrometer provides an extremely sensitive technique for determining the direct products of dissociation. However, the products of static experiments,[7,13] in which substrate pressures range from a few mTorr to hundreds of Torr, have usually been determined by gas chromatographic, infrared, and mass spectroscopic analyses of the gas mixture following photolysis by a few thousand laser pulses. More recently, a number of workers[14-17] have demonstrated the use of laser-induced fluorescence (LIF) and infrared detection techniques following chemiluminescent scavenging reactions to detect primary decomposition fragments 10^{-8}–10^{-5} sec after the laser pulse. For example, in some early IRMPD studies Houston,[16,17] Quick and Wittig,[18] and Preses *et al.*[19] were able to monitor HF emission after irradiating mixtures of SF_6 and various scavengers such as H_2 and HI with a CO_2 laser.

The trifluoromethyl halides are an excellent and very interesting class of molecules for studying the IRMPD process by the above techniques. Würzberg[13] *et al.* have observed IR fluorescence from both HF and HBr from the IRMPD of CF_3Br/HI mixtures. This observation alone would suggest a competitive two-channel dissociation mechanism. However, the additional observation of CF_2 by LIF indicates a two-step process in which CF_3 and Br are the primary products, and subsequent absorption of laser photons by CF_3 results in the formation of CF_2 and F:

$$CF_3Br + nh\nu \rightarrow CF_3 + Br\ ,$$

$$CF_3 + mh\nu \rightarrow CF_2 + F\ .$$

Secondary dissociation has been observed from the IRMPD of other systems, including SF_6,[20] SF_5Cl,[19] $CFCl_3$,[12] and C_2H_4.[15] In addition, CF_2 and F have also been observed from IRMPD of CF_3I,[13] indicating that the molecule undergoes secondary multiphoton photochemistry similar to CF_3Br. However, in the photolysis of CF_3Cl, Dever and Grunwald[7] observed stable products from the primary dissociation only, while Sudbø *et al.*, using an on-line mass spectrometer, observed no dissociation of CF_3 up to fluences of 50 J/cm^2.

With the current interest in parallel channel chemistry, a thorough understanding of secondary dissociation dynamics is important, especially to the interpretation of results from IRMPD studies.

In this work we report the observation of the Cl, F, and CF_2 photofragments produced by the infrared multiple photon dissociation of CF_3Cl. A secondary dissociation mechanism is proposed and a mechanism for the production of stable products is discussed.

II. EXPERIMENTAL

The experimental apparatus is shown in Fig. 1. The 4.1 J output from a Lumonics TEA-203 CO_2 TEA laser

[a)]Research carried out at Brookhaven National Laboratory under contract with the U. S. Department of Energy and supported, in part, by its Office of Basic Energy Sciences.
[b)]Research Collaborator, Brookhaven National Laboratory.

 0021-9606/81/095008-09$01.00

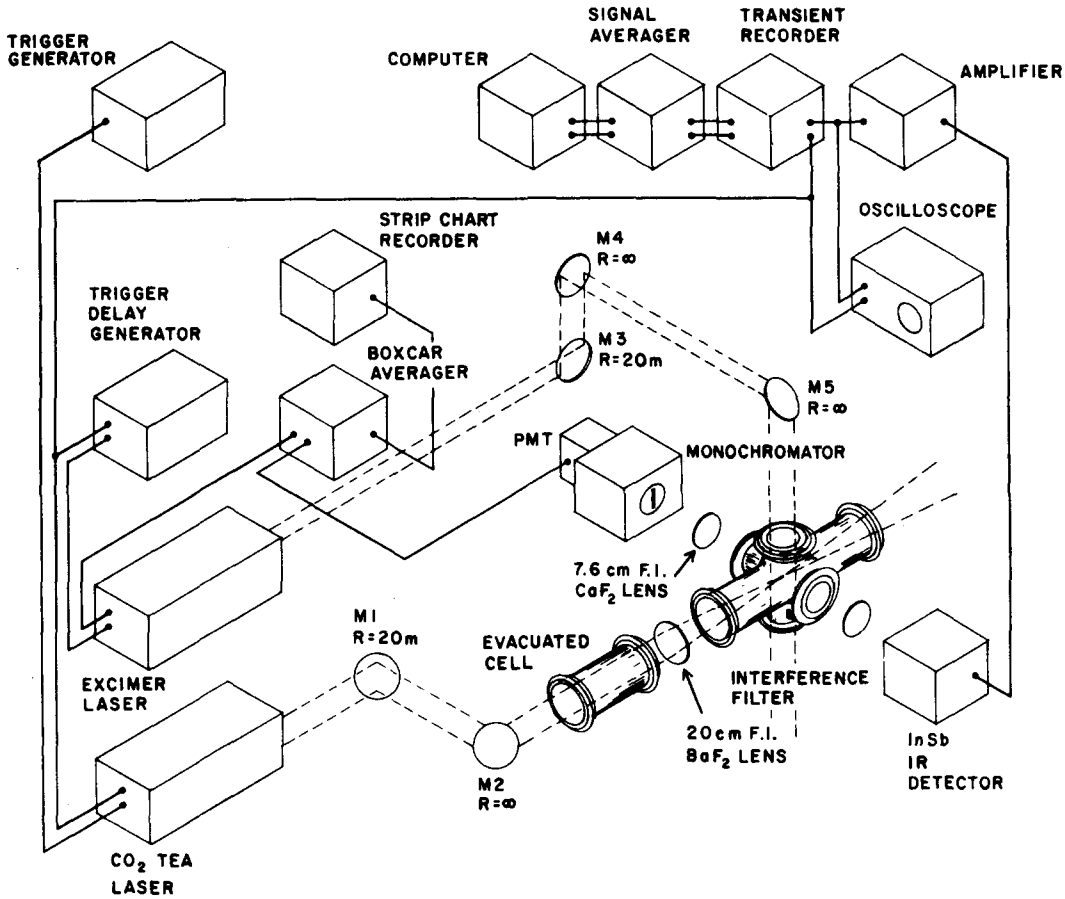

FIG. 1. Experimental apparatus. (1) Chemiluminescence studies: The focused output of a pulsed CO_2 TEA laser is used to dissociate CF_3Cl via IRMPD. A 20 cm long cell containing $CHCl_2F$ and argon is used to attenuate the laser beam. IR fluorescence from HCl or HF is monitored by an InSb 77 K detector. The detector output is amplified, digitized, signal averaged, and stored in a minicomputer. (2) Laser-induced fluorescence studies: The 249 nm output from a KrF laser, triggered 600 ± 100 nsec after the CO_2 laser, is directed into the photolysis cell perpendicular to the CO_2 laser beam. Laser-induced fluorescence is focused onto a 0.25 m monochromator and detected by a PMT. The PMT signals are boxcar averaged and printed on a strip chart recorder.

[100 nsec (FWHM) spike, tail ~3 μsec, partially mode locked and multitransverse mode] operating at 0.5 Hz was focused with a 20 cm focal length BaF_2 lens into a Pyrex sample cell, 4 cm diameter×40 cm long. Vacuum seals between the cell and the NaCl cell windows were made by Viton O rings coated with a protective film of Krytox fluorocarbon grease. A 20 cm long evacuated cell was placed in front of the BaF_2 lens to prevent dielectric breakdown of air resulting from focused laser light back-reflected from the cell windows. The laser beam waist at the center of the reaction cell was 2 mm in diameter,[15] resulting in peak laser fluences of ~140 J/cm². The beam exiting the cell was refocused by a 20 cm focal length BaF_2 lens, and a small fraction of the beam split off by a NaCl window and directed toward a Scientech energy meter. This fraction was determined by calibration against the total energy exiting the cell. Thus, the laser energy was accurately monitored for single pulses. Pressures of added gases were measured at the reaction cell with a Datametrics Barocel capacitance manometer (minimum sensitivity ≈ 10 ± 0.5 mTorr).

A. IR chemiluminescence

Cl and F atoms generated by the IRMPD of CF_3Cl were detected by the scavenging reactions

$$Cl + HBr \xrightarrow{k_1} HCl^{\dagger} + Br \ , \tag{1}$$

$$F + HBr \xrightarrow{k_2} HF^{\dagger} + Br \ . \tag{2}$$

(The dagger indicates vibrational excitation.) These reactions have been studied extensively in recent work, and the product vibrational distributions as well as the rate constants are well known.[16,17] IR chemiluminescence from $HCl^{\dagger}$ or $HF^{\dagger}$ was monitored at right angles to the laser beam with a 1.4 cm² Spectronics InSb photovoltaic detector situated 5 cm from the focal region of the cell. Within the detector field of view, the laser fluence varied by a factor of about 7. Narrow band interference filters (2.0–2.7 μm and 3.4–4.0 μm, FW at 10% max) were used to permit observation of emission from either $HCl^{\dagger}$ or $HF^{\dagger}$. The detector signals were amplified by factors of 10^3 to 10^6 with a detector-matched preamplifier from Spectronics and a Tektronix

AM502 amplifier. The amplified signals were then digitized by a Biomation 8100 Waveform Recorder (50–200 nsec/channel) and stored in a Tracor-Northern NS-570 signal averager. Signal-to-noise ratios for single events were typically ~ 1–5. Signal-averaged data were transferred to a PDP 11/34 computer for storage and analysis. The IR fluorescence signals were then fitted to a simple exponential rise and decay function using a three-parameter nonlinear least-squares fitting procedure.[25]

B. Laser-induced fluorescence

The $\tilde{A}\,^1B_1$ (0, 6, 0) ← $\tilde{X}\,^1A_1$ (0, 0, 0) and (0, 5, 0) ← (0, 0, 0) transitions of CF_2 were pumped by the output of a Lumonics 860S excimer laser operating on KrF at 249 nm (10 nsec FWHM). A trigger delay generator was used to pulse the KrF laser with a fixed delay relative to the CO_2 TEA laser pulse. The typical peak-to-peak delay between the CO_2 and excimer laser spikes in these experiments was ~600 ± 100 nsec. The 200–250 mJ output of the KrF laser was reduced to ~10–20 mJ by an aperture and directed into the cell through Suprasil windows at right angles to the CO_2 laser beam using a series of MgF_2-coated (2000 Å thick) aluminum mirrors. $\tilde{A}\,^1B_1 \rightarrow \tilde{X}\,^1A_1$ emission from CF_2 was then monitored through a Suprasil window at 90° to both laser beams. Emitted fluorescence was collected by a 7.6 cm focal length CaF_2 lens and imaged 1 : 1 onto the entrance slit of a 0.25 m Jarrell–Ash monochromator. With 1 mm or 150 μm fixed slits, spectral resolutions of ~ 2.5 and ~ 0.5 nm, respectively, were achieved. Calibration of the monochromator was performed using an Oriel Hg/Ar lamp. The spectrally resolved emission was detected by a 1P28 photomultiplier, the PMT signal averaged using a PAR 162 boxcar averager with model 164 plug-in (1 μsec time constant), and the integrated signals recorded on a Houston Instrument OmniScribe strip chart recorder.

Time-resolved emission was recorded by digitizing and signal averaging the PMT signals monitored at a single wavelength. The lifetime of the emission was extracted by fitting the data to a single exponential decay function using a nonlinear least-squares fit.[25]

C. CO_2 laser fluence studies

$HCl^\dagger$, $HF^\dagger$, and CF_2 production were studied as a function of CO_2 TEA laser fluence. Attenuation of the CO_2 laser beam was achieved by introducing mixtures of CCl_2FH and argon into the normally "evacuated cell" in Fig. 1. It was found that a mixture of 40 Torr of CCl_2FH and 60 Torr of argon attenuated the laser beam almost completely.

Data were acquired using the techniques described above with the following modifications. Each set of data was recorded for a single CO_2 laser pulse, and signal averaging was performed for only the lowest fluences in the $HCl^\dagger$ and $HF^\dagger$ chemiluminescence experiments. In the CF_2 study, a model 165 boxcar plug-in unit with variable sensitivity was used to facilitate detection of low fluorescence intensities for single shot experiments. All data were taken with the monochromator adjusted to transmit 257 nm light, corresponding to the strongest band in the observed CF_2 fluorescence spectrum. The value of the integrated signal for each pulse was then read directly from the boxcar digital display.

Gas chromatographic product analyses of irradiated samples were performed on a Varian 1520B gas chromatograph using an alumina column, 6.1 m × 0.32 cm, with He carrier at 100 °C, and a thermal conductivity detector operated at 150 °C.

All gases used in the experiments were research grade and, except for CF_3I (PCR), were purchased from Matheson. HBr was doubly distilled from a 4 : 1 pentane/isopentane/liquid N_2 slush at −138 °C. All other gases were degassed by several freeze (77 K)-pump-thaw cycles upon transfer to glass bulbs and were used without further purification. Argon was withdrawn from a liquid-nitrogen-cooled reservoir.

III. RESULTS

A. IR chemiluminescence

The kinetic solution for processes such as (1) and (2) has been discussed elsewhere.[18,19] It consists of a rapidly rising pseudo-first-order component followed by a slower exponential decay. Figure 2 shows signal-averaged fluorescence traces (32 shots) for processes (1) and (2). Typical traces have a signal-to-noise ratios ranging from 5 : 1 to 50 : 1 after signal averaging 16 to 256 laser pulses. Each figure shows clearly the fast rise due to formation of $HX^\dagger$ by the scavenging reaction as well as the V–T,R relaxation of the excited hydrogen halide that follows. The smooth line through the data represents the best nonlinear least-squares fit from which the exponential rise and decay constants are obtained. The major source of error in the computer fit arises from the difficulty in fixing the time origin of the fluorescence signal because of electronic noise from the CO_2 TEA laser discharge. However, the time origin does appear within the laser pulse. A nitrogen-lean laser gas mixture generates an output energy of ~ 60 J/cm^2 in a pulse shortened to ~ 50 nsec (FWHM) and without a tail. The resulting $HX^\dagger$ emission consistently originated within the laser pulse, indicating that processes occurring in the tail of the laser emission do not dominate the dissociation.

Time-resolved fluorescence from $HCl^\dagger$ and $HF^\dagger$ was monitored for various mixtures of CF_3Cl (0.01–0.33 Torr), HBr (0.026–0.31 Torr), and Ar(5–15 Torr), and the reaction rates were extracted from plots of the pseudo-first-order rate constant against HBr pressure (Fig. 3). The previously reported rate constants for reactions (1)[22] and (2)[16,17,21] are represented by the shaded areas. The rates measured in this work agree very well with the room temperature literature values, indicating the production of both chlorine and fluorine atoms in the IRMPD of CF_3Cl. Further evidence supporting the production of Cl and F atoms was obtained by substituting H_2 for HBr in the reaction mixture. Under these conditions, no perceptible $HCl^\dagger$ signal is detected since the reaction

$$Cl + H_2 \xrightarrow{k_3} HCl + H \qquad (3)$$

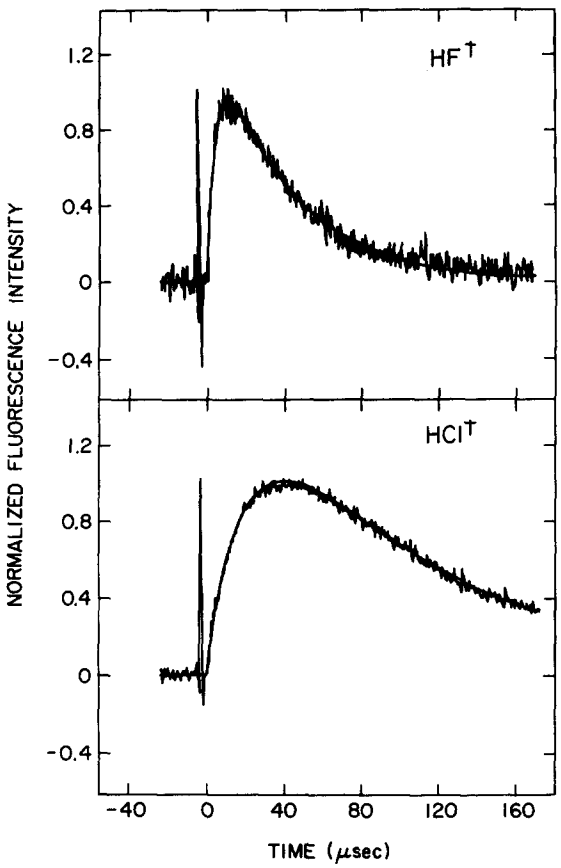

FIG. 2. $HCl^{\dagger}$ and $HF^{\dagger}$ signal-averaged (32 shots) IR fluorescence traces generated by photolyzing 33 mTorr CF_3Cl, 230 mTorr HBr, and 5 Torr Ar with the focused output of a CO_2 TEA laser operating on the R (40) line at 1090.03 cm^{-1}. Fluence is ~ 140 J/cm^2. The fast rise in each trace corresponds to the scavenging reaction (1) or (2), while $V-T$, R relaxation is observed in the slower decay that follows. Smooth lines through the data are the best nonlinear least-squares fits to the data.

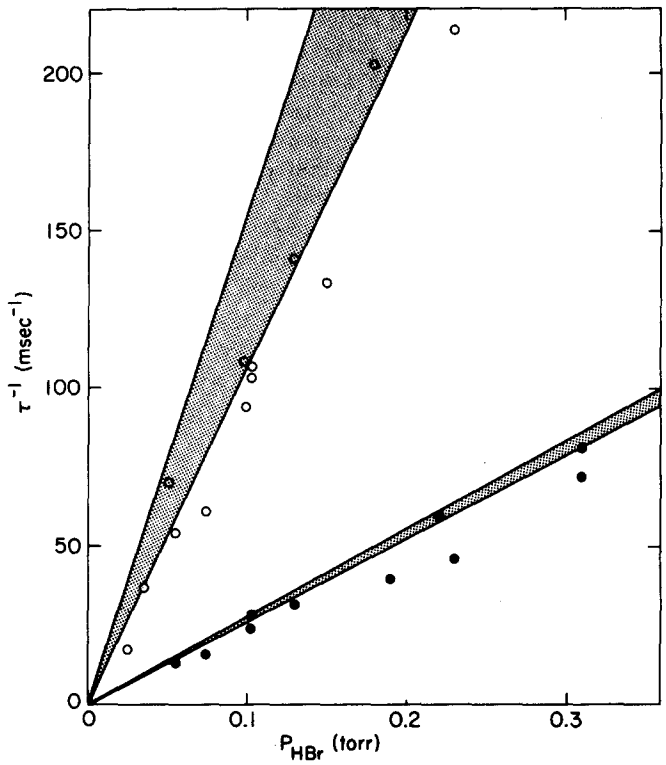

FIG. 3. Data for IRMPD chemiluminescent scavenging reactions. $HCl^{\dagger}$; ●: $HF^{\dagger}$:○. The shaded areas represent the range of previously measured rates.[16,17,21,22]

produces vibrationally cold HCl. In addition, the observed $HF^{\dagger}$ emission exhibits rise times in excellent agreement with the published rate constants[17] for the reaction

$$F + H_2 \xrightarrow{k_4} HF^{\dagger} + H \ . \qquad (4)$$

B. Laser-induced fluorescence

The spectrum shown at the top of Fig. 4 is the LIF spectrum generated from the products of the multiphoton dissociation of CF_3Cl. The LIF signal is observed only when the reaction cell contains CF_3Cl and the lasers are fired in the proper sequence. Blocking either laser beam results in complete loss of UV/visible emission. The band maxima and spacings in this spectrum correspond extremely well to those reported for CF_2 by King, Schenck, and Stephenson.[26] Since the ultimate resolution of our apparatus is lower than that generally achieved in spectroscopic studies, the LIF spectrum from a known source of CF_2 was generated for comparison. Stephenson and King[27] and Sudbø *et al.*[8] have demonstrated that as a result of IR multiphoton pumping, CF_2HCl undergoes HCl elimination and produces CF_2

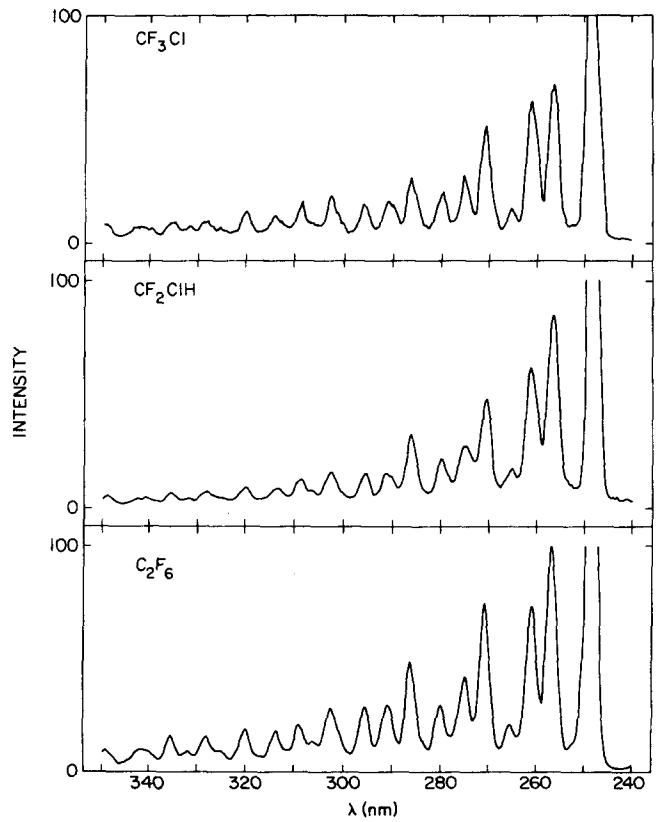

FIG. 4. Laser-induced fluorescence signals. For each trace, P_{Ar} = 15.00 Torr, P_{total} = 15.25 Torr. CO_2 laser conditions were as follows: CF_3Cl–R(40) line at 1090.03 cm^{-1}, fluence ~ 100 J/cm^2; CF_2HCl–R(26) line at 1082.30 cm^{-1}, fluence ~ 40 J/cm^2; C_2F_6–R(36) line at 1087.95 cm^{-1}, fluence ~ 83 J/cm^2.

in the ground electronic state. The center spectrum in Fig. 4 was obtained by LIF on our apparatus after dissociating CF_2HCl with the output of the CO_2 TEA laser operating on the $R(26)$ line of the 9.6 μm band. Agreement between this spectrum and that obtained from the decomposition of CF_3Cl is excellent. In addition, the radiative lifetime of the UV emission from each molecular fragmentation was measured for a number of peak wavelengths. The observed decay rates are self-consistent at all wavelengths, exhibiting no systematic variations. The measured overall lifetime is 58 ± 6 nsec, in excellent agreement with the radiative lifetime for the $\tilde{A}\,^1B_1$ state of CF_2 reported by King *et al.*[26]

Previous work[28] has shown CF_3 to be the only photoproduct generated in the IRMPD of C_2F_6 at low laser fluence. In order to demonstrate secondary dissociation of CF_3, we have studied the LIF spectrum of the decomposition products of C_2F_6 at high fluences using the $R(36)$ line of the 9.6 μm band of the CO_2 laser. The observed CF_2 spectrum generated from this system is displayed at the bottom of Fig. 4.

C. CO_2 laser fluence studies

When the nonlinear least-squares fitting procedure is applied to the signal-averaged IR chemiluminescence data, such as those in Fig. 2, three parameters are generated which together describe the observed time behavior accurately: k_{rise}, k_{fall}, and $[X]_0$. The parameters k_{rise} and k_{fall} correspond to the rapid rise and slow decay of the signal. The relative atom concentration at time zero, $[Cl]_0$ or $[F]_0$, is related to the CO_2 TEA laser fluence. Figure 5 shows the initial chlorine and fluorine atom concentrations plotted as a function of laser fluence from ~10 to 100 J/cm^2. The data have been normalized using the detector D^*_λ,[29] filter transmission and band pass,[30] radiative lifetimes,[31] and product state distributions.[23,24] No data were taken below 10 J/cm^2 because of poor detector sensitivity for $HF^\dagger$ and $HCl^\dagger$ IR emission. Over the range of fluences studied, the ratio $[Cl]_0 : [F]_0$ at a given fluence is ~3.5.

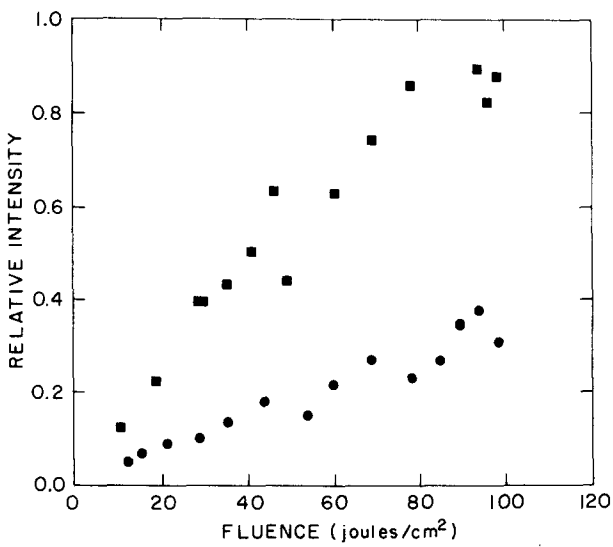

FIG. 5. Data for $HF^\dagger$ and $HCl^\dagger$ fluence studies. Intensities are normalized for D^*_λ, filter transmission and bandpass, radiative lifetime, and product state distributions. $HCl^\dagger$: ■; $HF^\dagger$: ●. Pressures are: $P_{CF_3Cl} = 0.02$ Torr, $P_{HBr} = 0.20$ Torr, $P_{Ar} = 10$ Torr.

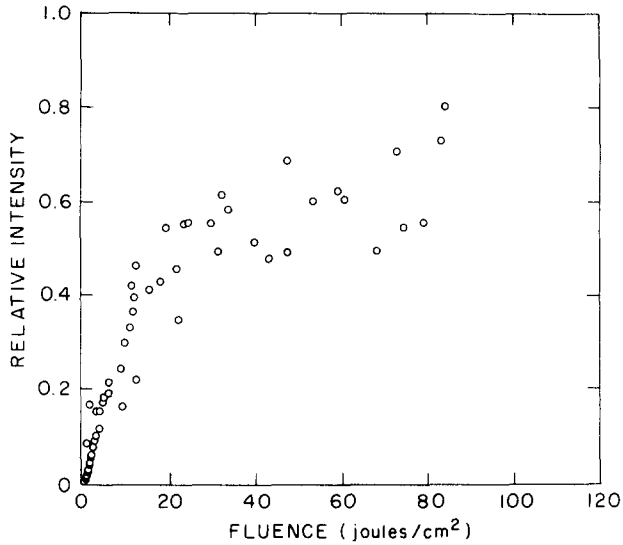

FIG. 6. CF_2 fluence study. Pressures are: $P_{CF_3Cl} = 0.25$ Torr, $P_{Ar} = 10$ Torr.

The production of CF_2 is plotted in Fig. 6 as a function of CO_2 laser fluence. The intensity, which rises rapidly at low CO_2 laser fluences, begins to level off at fluences ~10 J/cm^2, indicating the onset of saturation of the CF_2-producing dissociation mechanism. The results of a more precise study below saturation are shown in Fig. 7. From this plot it is difficult to determine the threshold for dissociation. However, our limit of detectability for the production of CF_2 is observed at ~0.6 J/cm^2.

D. Gas chromatographic product analysis

Assignment of peaks observed in the analyses of irradiated samples was achieved by comparisons of re-

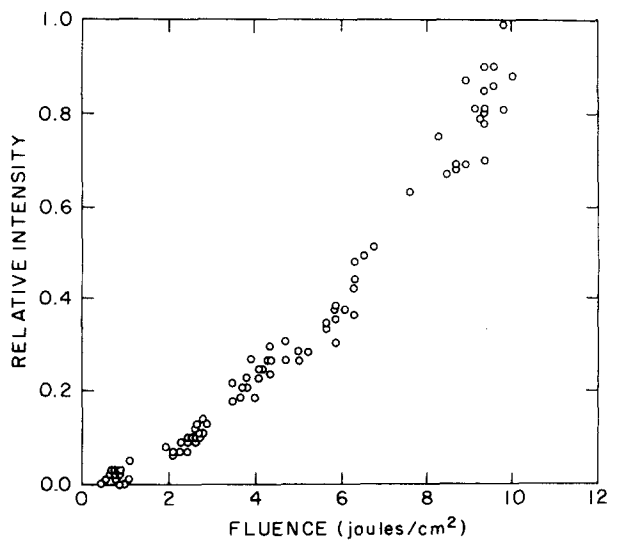

FIG. 7. CF_2 fluence study near threshold. Detectability of CF_2 on our apparatus is limited to fluences $\gtrsim 0.6$ J/cm^2. Pressures as in Fig. 6.

tention times on the column with those for pure gases. The major peaks observed in the gas chromatographic (GC) analysis of samples irradiated by 2000 laser pulses are due to CF_4, CF_2Cl_2, C_2F_6, and the parent molecule CF_3Cl. At low laser fluences (~ 0.2 J/cm^2), the photolysis products are present in a 1:1:1 ratio. As the fluence is increased, $[C_2F_6]$ increases linearly with fluence However, $[CF_4]$ and $[CF_2Cl_2]$ increase much more rapidly. At the highest fluences only CF_4 and CF_2Cl_2 appear as major product peaks in the GC analysis and are present in a 1:1 ratio.

IV. DISCUSSION

IR chemiluminescence and laser-induced fluorescence studies confirm the prompt formation of Cl, F, and CF_2 from multiphoton dissociation of CF_3Cl. Three mechanisms which may be invoked to explain these results are outlined in Table I.

Mechanism I is a competitive two-channel system in which generation of fluorine atoms requires that CF_3Cl absorb 12 CO_2 laser photons (38 kcal/mole) in excess of that required for dissociation via the lower energy channel. Figure 8 shows the RRKM rate constants for these two processes as a function of total internal energy. A discussion of this calculation can be found in the Appendix. Examination of Fig. 8 indicates that CF_3Cl molecules with sufficient internal energy to produce fluorine atoms (124 kcal/mole) will dissociate by this mechanism with a rate constant of 10^4 sec^{-1}. However, the rate constant for dissociation in the lower energy channel, generating chlorine atoms, is 10^{10} sec^{-1} at this internal energy. Thus, the observed ratio of Cl:F should be 10^6. The normalized $HCl^\dagger$ and $HF^\dagger$ data in Fig. 5 show that the ratio of Cl:F produced is ~ 3.5:1 over the range of fluences studied. It is unreasonable to assume that RRKM theory would be in error by six orders of magnitude. The major factor responsible for the large difference in rate constants is the 38 kcal/mole difference in critical energies for the two dissociation processes. Thus, it is more likely that another mechanism is responsible for fluorine atom generation. Furthermore, this dissociation scheme does not provide for the formation of CF_2.

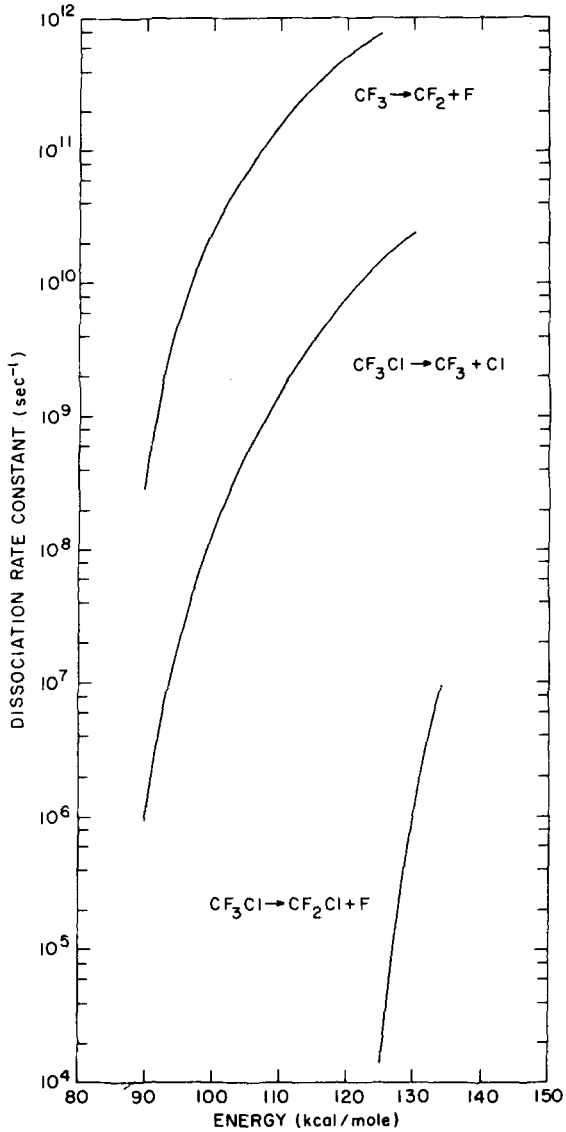

FIG. 8. RRKM calculation. See the Appendix.

TABLE I. Possible dissociation mechanisms.

Parallel dissociation channels		ΔH,[a] (kcal/mole)
I.	$CF_3Cl + nh\nu \rightarrow CF_3 + Cl$	86
	$+ mh\nu \rightarrow CF_2Cl + F$	124
II.	$CF_3Cl + nh\nu \rightarrow CF_3 + Cl$	86
	$+ mh\nu \rightarrow CF_2 + ClF$	111
Secondary dissociation		
III.	$CF_3Cl + nh\nu \rightarrow CF_3^\dagger + Cl$	86
	$CF_3^\dagger + mh\nu \rightarrow CF_2 + F$	88

[a]The endothermicities were calculated using the following heats of formation from Ref. 32: CF_3Cl, −169.2; CF_3, −112.4; CF_2, −43.5; ClF, −12.14; Cl, +28.92; F, +18.86. The value for CF_2Cl, −64, was estimated in Ref. 7.

The second mechanism outlined in Table I is also a two-channel scheme but requires less energy to open the second channel compared to mechanism I. However, the above argument can also be made against the possibility of this mechanism, since there is still a large difference in critical energies. In addition, since fluorine is produced in the form of ClF, the observed $HF^\dagger$ chemiluminescence signals should exhibit rise times representative of the reaction

$$ClF + HBr \xrightarrow{k_5} HF^\dagger + BrCl \ . \qquad (5)$$

In this study, the measured rise times agree very well with the known value[18,17,21] for the reaction F + HBr $\rightarrow$ $HF^\dagger$ + Br, as demonstrated in Fig. 3. It is extremely unlikely that the four-center exchange, Reaction (5), produces vibrationally excited $HF^\dagger$ with the same rate of reaction. In fact, HF and BrCl are not even the thermodynamically favored products for Reaction (5).[32]

The final mechanism suggested in Table I is a se-

TABLE II. RRKM calculation[a] for dissociation of CF_3Cl.

Number of excess photons	Excess energy (kcal/mole)	Average translational energy (kcal/mole)	Average vibrational energy (kcal/mole)	Average velocity of Cl (10^4 cm/sec)
1	3.11	0.82	2.29	3.57
2	6.22	1.26	4.96	4.43
3	9.33	1.63	7.70	5.04
4	12.44	1.98	10.46	5.55
5	15.55	2.32	13.23	6.01

[a]See the Appendix.

quential dissociation process in which CF_3 and Cl are the primary products. Vibrationally excited CF_3 then undergoes secondary dissociation by subsequent multiphoton absorption, generating CF_2 and F. The data collected here support this argument. For example, the observed rate for the formation of $HCl^{\dagger}$ via Reaction (1) indicates that Cl atoms are produced with nearly thermal velocity (4.22×10^4 cm/sec). Table II lists the results of our RRKM calculation for the unimolecular decomposition of CF_3Cl. The data indicate that Cl atoms with thermal velocities are generated from CF_3Cl molecules with an energy above the dissociation threshold corresponding to two excess laser photons. Sudbø *et al.*[12] have studied the angular distribution of CF_3 generated from CF_3Cl in the MPD process. These workers have shown that their data agree with RRKM calculations incorporating 0.5–1.5 laser photons above the dissociation energy. This concurs with our result and indicates (from Fig. 8) that CF_3Cl molecules dissociate after absorbing 1–2 photons in excess of threshold. The lifetime predicted for this process is 200–800 nsec. CF_3 formed in such a decomposition would thus contain 2.3–5 kcal/mole of vibrational energy. Würzberg *et al.*[13] have studied the IRMPD of CF_3Br and calculate that decomposition occurs from vibrational levels two to three quanta above the dissociation limit. This results in formation of CF_3 fragments with 6.0–8.8 kcal/mole internal energy, a region corresponding to the "quasicontinuum."[13] By analogy, CF_3 generated from CF_3Cl is expected to be born near to, if not in, the quasicontinuum, and therefore will be easily pumped by the CO_2 laser. In addition, the CF_3 symmetric stretch occurs at 1087 cm^{-1},[33,34] which is certainly near enough to the laser frequency (1090 cm^{-1}) for resonant absorption to occur below the quasicontinuous levels. For CF_3 and CF_3Cl internal energies of 90 kcal/mole, the RRKM calculation in Fig. 8 predicts that the rate for secondary dissociation of CF_3 forming CF_2 and F is 250 times faster than decomposition of the parent molecule to CF_3 and Cl. This is consistent with the observation from the chemiluminescence studies that similar quantities of Cl and F are generated in the IRMPD process.

The validity of mechanism III is crucially dependent upon the multiphoton absorption and dissociation characteristics of CF_3. Fisk[28] has demonstrated that C_2F_6 will undergo C–C bond scission when pumped by the $R(36)$ line of the 9.6 μm band of a CO_2 laser. At fluences below 6 J/cm^2 the only photolysis product detected is CF_3. Attempts to monitor chemically CF_2 formation produced negative results. However, using laser-induced fluorescence we have observed CF_2 production from the IRMPD of C_2F_6 at much higher fluences. The bottom scan in Fig. 4 shows the LIF spectrum of CF_2 observed at a laser fluence of ~80 J/cm^2. The similarity between this scan and the spectra monitored in the photolysis of CF_2HCl and CF_3Cl clearly demonstrates the IR multiphoton dissociation of CF_3 as well as the phenomenon of secondary dissociation.

If mechanism III correctly describes the multiphoton dissociation dynamics of CF_3Cl, then CF_2 and F are generated simultaneously in the secondary dissociation of CF_3 and only in this manner. Consequently, measurements of the kinetic parameters for CF_2 and F will provide a strong test for the validity of the mechanism. For example, the dependence of CF_2 and F atom production on CO_2 laser fluence should be identical. Unfortunately, we are unable to make this comparison because of the different detection geometries for the two experiments. While the CF_2 studies sample a 1 mm wide region at the center of the focus, our $HF^{\dagger}$ investigation measures IR fluorescence from an area extending 5–7 cm along the IR beam. It is reasonable, then, that while the CF_2 fluence curve begins to exhibit saturation above fluences of ~10 J/cm^2, the $HF^{\dagger}$ fluence curve should continue to rise, as we observe. The latter occurs because the regions to either end of the focus become more important to the total fluorescence signal as the laser fluence is increased. Attempts to sample the IR emission in the same geometry as the LIF signals failed due to poor detector sensitivity for IR photons compared to that for detection of UV/visible light.

A final piece of evidence supporting mechanism III is given by the stable product analysis. A simple set of reactions may be invoked to explain the formation of the observed products assuming the dissociation scheme of mechanism III. This scheme is less complicated than that postulated by Dever and Grunwald,[7] for example. The scheme outlined in Table III considers only radical recombination reactions. At relatively low fluences, the stable products C_2F_6, CF_4, and CF_2Cl_2 were detected in a 1:1:1 ratio, consistent with the stochiometry of this reaction scheme. At higher fluences, $[C_2F_6]$ increased, but $[CF_4]$ and $[CF_2Cl_2]$ increased much more rapidly. This can be understood in terms of the increasing importance of secondary dissociation at higher fluences. The rate of Reaction (4) in Table III rises with increasing fluence relative to Reaction (1) as indicated in Fig. 8. Consequently, the rates of Reactions (5), (6), and (7) will increase relative to the rate of

TABLE III. Possible reaction scheme leading to stable products.

$4CF_3Cl + nh\nu \rightarrow 4CF_3 + 4Cl$	(1)
$2CF_3 \rightarrow C_2F_6$ [a]	(2)
$2Cl + M \rightarrow Cl_2 + M$ [b]	(3)
$CF_3 + mh\nu \rightarrow CF_2 + F$	(4)
$CF_3 + F \rightarrow CF_4$ [c]	(5)
$CF_2 + Cl \rightarrow CF_2Cl$ [d]	(6)
$CF_2Cl + Cl \rightarrow CF_2Cl_2$ [e]	(7)
$4CF_3Cl + (n+m)h\nu + M \rightarrow C_2F_6 + CF_4 + CF_2Cl_2 + Cl_2 + M$	

[a] $\Delta H = -96$ kcal/mole[32]; $k = 4\times10^{-11}$ cm^3 molecule^{-1} sec^{-1}.[35]
[b] $\Delta H = -58$ kcal/mole[32]; $k = 4\times10^{-15}$ cm^3 molecule^{-1} sec^{-1}.[36]
[c] $\Delta H = -130$ kcal/mole[32]; $k = 1\times10^{-9}$ cm^3 molecule^{-1} sec^{-1}.[37]
[d] $\Delta H = -49$ kcal/mole[7,32]; $k = 1\times10^{-9}$ cm^3 molecule^{-1} sec^{-1}.[37]
[e] $\Delta H = -82$ kcal/mole[7,32]; $k = 1\times10^{-9}$ cm^3 molecule^{-1} sec^{-1}.[37]

reaction (2). This results in a stronger fluence dependence for production of CF_4 and CF_2Cl_2 compared to C_2F_6, consistent with the observations.

The reaction sequence suggested here is not the only mechanism which adequately accounts for the products. However, a simple and concise scheme which neglects the secondary IRMPD of CF_3 in the dissociation mechanism is not possible.

V. CONCLUSION

CF_2, Cl, and F have been detected as direct products of the IR multiphoton dissociation of CF_3Cl. These observations are consistent with a two-step mechanism in which CF_3 and Cl are the primary products. Vibrationally excited CF_3 then undergoes secondary dissociation by subsequent multiphoton absorption, generating CF_2 and F. RRKM calculations of the unimolecular dissociation rates for CF_3Cl and CF_3 indicate that CF_3Cl dissociates from levels two photons above threshold with a dissociation lifetime of ~200 nsec. The CF_3 radical with one photon of excess internal energy above the threshold for C–F bond cleavage is calculated to dissociate 100 times faster. IR multiphoton dissociation of CF_3 has been demonstrated by the observation of CF_2 in the IRMPD of C_2F_6 at high laser fluence.

A simple reaction scheme has been suggested which accounts for the formation of all observed stable products as well as their relative abundances at high and low laser fluence. Much more complicated reaction pathways must be invoked if secondary dissociation of CF_3 is not assumed.

ACKNOWLEDGMENT

We wish to thank Dr. C. R. Quick, Jr. for some helpful comments and valuable experimental advice.

APPENDIX: RRKM CALCULATIONS

Rate constants for the unimolecular dissociation $CF_3Cl \rightarrow CF_3 + Cl$, $CF_3Cl \rightarrow CF_2Cl + F$, and $CF_3 \rightarrow CF_2 + F$ were calculated using the RRKM method. The Bunker–Hase computer program[38] was used for this purpose.

For the dissociation of CF_3Cl to CF_3 and Cl, the following parameters were used in this calculation: (a) molecular vibrational frequencies in cm^{-1} (degeneracies in parentheses)[39]: 1105, 781, 476, 1212(2), 563(2), 350(2); (b) vibrational frequencies of the activated complex[40]: 1105, 320, 1212(2), 400(2), 350(2); (c) critical energy[32]: 86 kcal/mole.

All rotations were treated as inactive, vibrations were treated as harmonic, and no centrifugal corrections were made. The densities of states were calculated using the Whitten–Rabinovitch approximation,[41] which was also used for calculating sums of states for excess energies 10 kcal/mole and more above the critical energy. A direct-count method was used to evaluate sums of states at lower energies; the differences between these and the results from the Whitten–Rabinovitch approximation are negligible at excess energies greater than 4 kcal/mole.

This same calculation gave values of the distribution function $P(E_t)$ for the translational energy of the dissociation fragments. Numerical integration was used to obtain the average translational energy from $P(E_t)$.

It should be noted that Sudbø *et al.*[12] have carried out similar calculations which differ in several details from ours. They used a considerably lower critical energy, 81.5 kcal/mole. The frequency used for the vibration that becomes the reaction coordinates was 560 cm^{-1}, whereas the C–Cl stretching mode has a frequency of 781 cm^{-1}. The major difference, however, is in their assumption of a very "loose" complex, with a C–Cl bond stretched to almost three times its original length and C–Cl bending mode frequencies reduced to 21 cm^{-1} in the activated complex. As a result, the preexponential term in their rate constant is much larger than ours, and in the pertinent energy range, their values of $k(E)$ are larger by roughly two orders of magnitude.

Unfortunately, experimental data for unimolecular dissociations of alkyl halides are few and far between and, as a result, we are unable to determine the best model on the basis of comparison with experiment. Danilov *et al.*[42] determined the Arrhenius parameters for the dissociation of CF_3I and obtained a preexponential factor of 2.5×10^{15} sec^{-1}, which is in the range of those predicted with a "loose" complex. However, the temperature control in their experiments was poor and they were probably performed in the falloff pressure region. For our present purposes, the important points to be made on the basis of RRKM calculations are the relative rates of the two possible dissociation reactions of CF_3Cl, the relative rate of dissociation of CF_3, and the energy distribution in the fragments. These quantities should be relatively insensitive to the absolute values of the rate constants.

For the alternative dissociation channel of CF_3Cl to F atoms and CF_2Cl, the parameters were: (a) the same molecular vibrational frequencies; (b) vibrational frequencies of the activated complex[43]: 1212, 1105, 781, 400(2), 340(3); (c) critical energy[32]: 124 kcal/mole.

The reaction path degeneracy was three, and the sums of states were evaluated by direct count. Other details of the calculation are the same as those discussed above.

Calculations for CF_3 dissociation were made with the following input data: (a) molecular frequencies[33,34]: 1090, 700, 1260(2), 510(2); (b) vibrational frequencies of the activated complex[43]: 1260, 1090, 550, 400(2); (c) critical energy[32]: 87.8 kcal/mole.

The reaction path degeneracy was three, and a direct-count method was used to evaluate sums of states. Other details were the same as those described above.

[1]P. A. Schulz, Aa. S. Sudbø, D. J. Krajnovich, H. S. Kwok, Y. R. Shen, and Y. T. Lee, Annu. Rev. Phys. Chem. **30**, 379 (1979).

[2]N. Bloembergen and E. Yablonovitch, Phys. Today **31**, 23 (1978).

[3]R. V. Ambartzumian and V. S. Letokhov, in *Chemical and Biochemical Applications of Lasers*, edited by C. B. Moore (Academic, New York, 1977), Vol. III, Chap. 2.

[4]R. V. Ambartzumian, V. S. Letokhov, E. A. Ryolov, and N. V. Chekalin, JETP Lett. **20**, 273 (1974).

[5]K. M. Leary, J. L. Lyman, L. B. Asprey, and S. M. Freund, J. Chem. Phys. **68**, 1671 (1978).

[6]I. P. Herman and J. B. Marling, Chem. Phys. Lett. **64**, 75 (1979).

[7]D. F. Dever and E. Grunwald, J. Am. Chem. Soc. **98**, 5055 (1976).

[8]Aa. S. Sudbø, P. A. Schulz, Y. R. Shen, and Y. T. Lee, J. Chem. Phys. **69**, 2312 (1978).

[9]A. Kaldor, R. B. Hall, D. M. Cox, J. A. Horsley, P. Rabinowitz, and G. M. Kramer, J. Am. Chem. Soc. **101**, 4465 (1979).

[10]D. S. King and J. C. Stephenson, Chem. Phys. Lett. **51**, 48 (1978).

[11]R. J. S. Morrison and E. R. Grant, J. Chem. Phys. **71**, 3537 (1979).

[12]Aa. S. Sudbø, P. A. Schulz, E. R. Grant, Y. R. Shen, and Y. T. Lee, J. Chem. Phys. **70**, 912 (1979).

[13]E. Würzberg, L. J. Kovalenko, and P. L. Houston, Chem. Phys. **35**, 317 (1978).

[14]J. C. Stephenson and D. S. King, J. Chem. Phys. **69**, 1485 (1978).

[15]C. R. Quick, Jr., A. B. Horwitz, R. E. Weston, Jr., and G. W. Flynn, Chem. Phys. Lett. **72**, 352 (1980).

[16]E. Würzberg, A. J. Grimley, and P. L. Houston, Chem. Phys. Lett. **57**, 373 (1978).

[17]P. L. Houston, Adv. Chem. Phys. (to be published).

[18]C. R. Quick, Jr. and C. Wittig, Chem. Phys. Lett. **48**, 420 (1977).

[19]J. M. Preses, R. E. Weston, Jr., and G. W. Flynn, Chem. Phys. Lett. **48**, 425 (1977).

[20]E. R. Grant, M. J. Coggiola, Y. T. Lee, P. A. Schulz, Aa. S. Sudbø, and Y. R. Shen, Chem. Phys. Lett. **52**, 595 (1977).

[21]E. Würzberg and P. L. Houston, J. Chem. Phys. **72**, 5915 (1980).

[22]C.-C. Mei and C. B. Moore, J. Chem. Phys. **67**, 3936 (1977).

[23]D. Brandt, L. W. Dickson, L. N. Y. Kwan, and J. C. Polanyi, Chem. Phys. **39**, 189 (1979).

[24]D. H. Maylotte, J. C. Polanyi, and K. B. Woodall, J. Chem. Phys. **57**, 1547 (1972).

[25]P. R. Bevington, *Data Reduction and Error Analysis for the Physical Sciences* (McGraw-Hill, New York, 1969), Chap. 11.

[26]D. S. King, P. K. Schenck, and J. C. Stephenson, J. Mol. Spectrosc. **78**, 1 (1979).

[27]J. C. Stephenson and D. S. King, J. Chem. Phys. **69**, 1485 (1978).

[28]G. A. Fisk, Chem. Phys. Lett. **60**, 11 (1978).

[29]H. Melchior, M. B. Fisher, and F. R. Arams, in *Infrared Detectors*, edited by R. D. Hudson and J. W. Hudson (Dowden, Hutchinson and Ross, Stroudsburg, 1975), p. 97.

[30]Transmission curves were supplied by Optical Coating Laboratories, Inc. (OCLI) with interference filters.

[31]J. M. Herbelin and G. Emanuel, Aerospace Report No. TR-0074(4530)-5 (1974).

[32]D. R. Stull and H. Prophet, "JANAF Thermochemical Tables," edited by D. R. Stull and H. Prophet 2nd ed. Natl. Stand. Ref. Data Ser. Natl. Bur. Stand. **37** (1971); M. W. Chase, J. L. Curnutt, A. T. Hu, H. Prophet, A. N. Syverud, and L. C. Walker, J. Phys. Chem. Ref. Data **3**, 311 (1974); M. W. Chase, J. L. Curnutt, H. Prophet, R. A. McDonald, and A. N. Syverud, *ibid.* **4**, 1 (1975); M. W. Chase, Jr., J. L. Curnutt, R. A. McDonald, and A. N. Syverud, *ibid.* **7**, 793 (1978).

[33]D. E. Milligan and M. E. Jacox, J. Chem. Phys. 48, 2265 (1968).

[34]G. A. Carlson and G. C. Pimentel, J. Chem. Phys. **44**, 4053 (1966).

[35]A. P. Stefani, in *Fluorine Chemistry Reviews*, edited by P. Tarrent (Dekker, New York, 1971), Vol. 5, p. 115.

[36]R. T. Watson, J. Phys. Chem. Ref. Data **6**, 871 (1977).

[37]The rate constant for CF_3+F was calculated for hard-sphere collisions, using collision diameters for CF_4 and Ne. See H. S. Johnston, *Gas Phase Reaction Rate Theory* (Ronald, New York, 1966), p. 153. The other radical+atom rate constants were assumed to be the same.

[38]W. L. Hase and D. L. Bunker, Program No. 234 Quantum Chemistry Program Exchange, University of Indiana, Bloomington, Ind. 47401.

[39]T. Shimanouchi, J. Phys. Chem. Ref. Data **3**, 285 (1974).

[40]I. Oref and B. S. Rabinovitch, J. Phys. Chem. **81**, 2587 (1977).

[41]G. Z. Whitten and B. S. Rabinovitch, J. Chem. Phys. **38**, 2466 (1963).

[42]O. B. Danilov, V. V. Elagin, V. Yu Zalesskii, and I. L. Yachnev, Kinet. Katal. **16**, 302 (1975).

[43]A degenerate C–F stretching mode was chosen as the reaction coordinate. The changes in other frequencies were analogous to those used for the F_3C–Cl activated complex.